Colloid Polym Sci 277:15–24 (1999)


ORIGINAL CONTRIBUTION

R.M. Clapperton
R.H. Ottewill
A.R. Rennie
B.T. Ingram

# Comparison of the size and shape of ammonium decanoate and ammonium dodecanoate micelles

Received: 27 July 1998
Accepted: 18 August 1998

R.M. Clapperton[1] · R.H. Ottewill (✉)
A.R. Rennie[2]
School of Chemistry University of Bristol
Bristol BS8 ITS, UK

B.T. Ingram
Procter and Gamble Limited
Newcastle Technical Centre, Longbenton
Newcastle-upon-Tyne NE12 9TS, UK

*Present addresses*:
[1]Albright and Wilson, Warley,
West Midlands, UK
[2]Industrial Materials Group, Department
of Crystallography, Birkbeck College,
Malet Street, London WC1E 7HX, UK

**Abstract** The size and shape of ammonium decanoate and ammonium dodecanoate micelles as functions of micellar concentration have been studied using the techniques of small-angle neutron scattering and time-averaged light scattering. The results indicate that the micellar mass of ammonium dodecanoate increases with surfactant concentration. This behaviour can be attributed to the formation of rod-like micelles. A comparison is made with the homologous surface active agent, ammonium decanoate.

**Key words** Light scattering – Small-angle neutron scattering – Ammonium decanoate – Ammonium dodecanoate – Cylindrical micelles

## Introduction

There are several factors which are known to influence the preferred size and shape adopted by surfactants. These include the alkyl chain length [1], the number of alkyl chains per molecule [1], the nature of the headgroup [1], counterion type [2, 3], alkyl chain flexibility [4–6], surfactant concentration [2, 7, 8] and electrolyte concentration [9, 10]. In general, spherical micelles are favoured by surfactants possessing a single, short alkyl chain in combination with a large headgroup at low electrolyte concentrations; for example, sodium dodecyl sulphate in water [9]. Tanford [1] describes how alternative micellar shapes such as the capped rod or rounded disc can accommodate more surfactant molecules per micelle than a regular sphere and this explains commonly observed micellar masses which exceed those expected for spheres. Enlarged micelles are favoured by an increase in electrolyte concentration; for instance, the sphere-to-rod transition of sodium dodecyl sulphate at 0.6 mol $dm^{-3}$ added salt [9]. Also, within a homologous series, an increase in alkyl chain length is frequently associated with an increase in aggregation number [1]. In conditions which favour the formation of enlarged micelles, an increase in micelle size with surfactant concentration is often observed. Growth of rod-like micelles has thus been reported for hexadecyltrimethyl ammonium bromide [11] and for sodium dodecyl sulphate [9, 12, 13].

This work in combination with previous studies [5] reports the effect of alkyl chain length on micellar shape for the ammonium salts of linear saturated fatty acids, and gives a comparison with other anionic surfactants. For example, in $NH_4OH$-$NH_4Cl$ buffered solutions at an ionic strength of 0.1, ammonium octanoate and ammonium decanoate (AmDec) have been shown [5] by small-angle neutron scattering (SANS) to form spherical micelles. AmDec maintains a constant micellar mass above the critical micelle concentration (cmc) over the micellar concentration range 0.06–0.1 mol $dm^{-3}$. The behaviour of ammonium dodecanoate (AmDodec) micelles under similar conditions is now reported.

This work forms an extension of previous work on the properties of mixtures of ammonium alkanoates and ammonium perfluoro-octanoate (APFO) [14–17] and forms a precursor to the examination of AmDodec-APFO mixtures by scattering methods [18].

## Experimental

### Materials

All water used was doubly distilled from an all-Pyrex still. Dodecanoic acid and decanoic acid were Fluka puriss grade material with an estimated gas-liquid chromatographic purity of >99%. The acids were converted to the ammonium salt by slow neutralisation of aqueous solutions with ammonium carbonate (BDH Analar grade material stabilised by ammonium carbamate) and then buffered by addition of $NH_4Cl$, to give a pH of 9.2 for AmDec and 9.8 for AmDodec at an ionic strength of 0.1.

### SANS measurements

Measurements were made at the Institut Laue Langevin (ILL), Grenoble, using the neutron diffractometer D17 [19]. The surface active agent solutions were contained in optical quality quartz cells having a path length of 1 mm. The scattering measurements were carried out using sample-to-detector distances of 1.40 and 2.80 m and an incident neutron beam wavelength of 10.0 Å; the full width at half-height of the distribution of wavelengths, $\Delta\lambda/\lambda$, was 10%.

Measurements were made over a scattering vector, $Q$, range from 0.01 to 0.21 $Å^{-1}$ with $Q$, for elastic scattering, defined as;

$$Q = 4\pi n \sin(\theta/2)/\lambda$$

where $n$ is the refractive index, $\lambda$ is the wavelength of the radiation in the medium and $\theta$ is the scattering angle; for neutrons the refractive index can be taken as unity.

Standard ILL programs were used to calculate the intensity as a function of $Q$ and to subtract the background arising from the cell and dispersion medium in order to make allowance for the attenuation of the beam by the sample. A 1 mm $H_2O$ sample was used to normalise the data for relative detector efficiences and to determine the absolute intensity. Data was converted to an absolute differential scattering cross-section, $d\Sigma(Q)/d\Omega$, using the scattering cross-section of water at 10 Å as given by Jacrot [20].

### Time-averaged light scattering (TLS) measurements

Measurements were made using a Brice Phoenix universal light scattering photometer, type OM-2000 [21], employing unpolarised blue light of wavelength 436 nm (in air). This instrument was found useful for weakly scattering samples since the volume of sample from which the scattered light was collected was relatively large. Since the variation of intensity with angle for these samples was small, measurements of intensity were made at 90° ($I_{90}$). For light scattering $\theta = 90°$ corresponded to a $Q$ value of 0.0027 $Å^{-1}$. The $I_{90}$ values were converted into absolute turbidity units, $\tau$, using the equation

$$\tau = CI_{90},$$

where $C$ is an instrument calibration constant; this was determined using purified benzene as a liquid with a known turbidity of $7.794 \times 10^{-4}$ $cm^{-1}$ at 436 nm [22, 23].

All materials were checked to ensure the absence of fluorescent impurities and in order to avoid contamination from dust particles all solutions were filtered through 0.2 $\mu$m Millipore filters. A measured dissymmetry ratio of $I_{60}/I_{120}$ of less than 1.05 was taken to indicate a dust-free sample.

Specific refractive index increments, $dn/dc$, were determined using a differential refractometer at a wavelength (in air) of 436 nm. The instrument was calibrated using aqueous KCl solutions as standards [24]. The values for AmDec and AmDodec are listed in Table 1.

## Results

### Time-average light scattering

The scattering results obtained for AmDec and AmDodec are shown in Fig. 1 as plots of turbidity, $\tau$ against the total concentration of surfactant. As can be seen, for both materials, $\tau$ decreases with decreasing concentration towards the cmc of the surfactant and then levels out below the cmc. The cmc values obtained from the light scattering results were 0.055 and 0.00925 mol $dm^{-3}$; in previous work the cmc values were found to be 0.041 mol $dm^{-3}$ from surface tension [15] and 0.0092 mol $dm^{-3}$ from nmr, [17] for AmDec and

**Table 1** Physical parameters of AmDec and AmDodec

| Formula | Molecular mass /g $mol^{-1}$ | $dn/dc$ /$cm^3$ $g^{-1}$ |
|---|---|---|
| $C_9H_{19}COONH_4$ | 189.18 | 0.141 |
| $C_{11}H_{23}COONH_4$ | 217.21 | 0.160 |

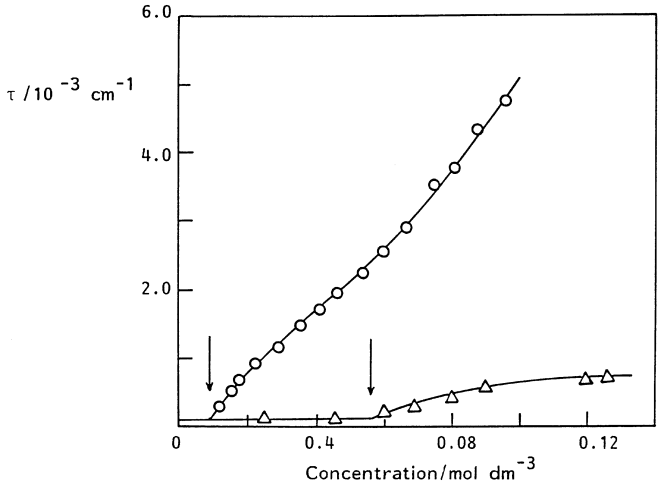


**Fig. 1** Turbidity against concentration for AmDec (△) (pH = 9.2, $I$ = 0.1) and AmDodec (○) (pH 9.8, $I$ = 0.1). The *arrows* indicate the critical micelle concentration

AmDodec respectively. An interesting feature of the curves is that with AmDec the turbidity reaches a plateau with increasing concentration and then decreases slightly as found previously [2]. However, with AmDodec the turbidity initially behaves similarly to AmDec and many other surfactants [2, 25] but then changes gradient followed by an increase in $\tau$ as the concentration increases.

The scattering from the micellar species was taken as $\tau - \tau_0$ with the scattering below the cmc denoted as $\tau_0$. The concentration of micellar species was taken as $C - C_0$ with $C$ = the total concentration of surfactant species and $C_0$ the cmc value. The results thus obtained are shown in Fig. 2 in the form of $(C - C_0)/(\tau - \tau_0)$ against $(C - C_0)$. The micellar mass $M_{\text{mic}}$ was calculated from [2, 25],

$$H(C - C_0)/(\tau - \tau_0) = 1/M_{\text{mic}} + 2B(C - C_0) \quad (1)$$

$H$, an optical constant, was taken as,

$$H = 32\pi^3 n_0^2 (\mathrm{d}n/\mathrm{d}c)^2 / 3N_{\text{AV}}\lambda_0^4 \quad (2)$$

**Table 2** Light Scattering $M_{\text{mic}}$ results

| Surfactant | cmc/mol dm$^{-3}$ | $H$/cm$^2$ g$^{-2}$ mol | $M_{\text{mic}}$/g mol$^{-1}$ |
|---|---|---|---|
| AmDec | $5.50 \times 10^{-2}$ | $5.427 \times 10^{-6}$ | 10 200 ± 1000 |
| AmDodec | $9.25 \times 10^{-3}$ | $6.989 \times 10^{-6}$ | 57 800 ± 3000 |

with $n_0 = 1.3401$, the refractive index of water at 436 nm [26], $N_{\text{AV}}$ = Avogadro's number and $(\mathrm{d}n/\mathrm{d}c)$ from Table 1. $B$ is the osmotic second virial coefficient.

The results obtained by extrapolation to zero $(C - C_0)$ are given in Table 2. A noticeable difference occurs in the behaviour of the curves in Fig. 2. For AmDec the curve has an overall small positive slope, whereas in the case of AmDodec the curve has a small positive slope at the lower $(C - C_0)$ values then goes through a maximum and at the higher $(C - C_0)$ values has a negative slope. The latter effect could be interpreted as an increase of attraction between the micelles, or alternatively as an increase in micellar mass with increasing concentration of surfactant (see later).

*SANS measurements*

SANS results are reported for AmDec and AmDodec in $NH_4Cl$-$NH_4OH$ buffer in $D_2O$ at an ionic strength of 0.1 and at pH values of 9.2 and 9.8, respectively. These conditions were the same as those used for light scattering experiments.

For a monodisperse system of non-interacting micelles the differential scattering cross-section as a function of $Q$ is given by the expression,

$$\mathrm{d}\Sigma(Q)/\mathrm{d}\Omega = V_p^2 N_p (\rho_p - \rho_m)^2 P(Q), \quad (3)$$

where $N_p$ = number of micelles per cubic centimetre, $V_p$ = the volume of each micelle and $P(Q)$ is the particle shape factor. $\rho_p$ is the coherent neutron scattering length density of the micellar unit and $\rho_m$ is the coherent neutron scattering density of the dispersion medium. For a homogeneous sphere of radius $R$, $P(Q)$ is given by [27],

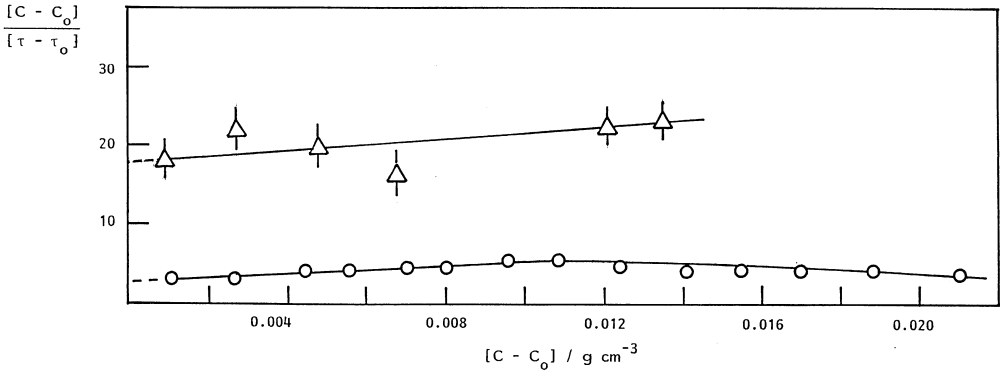


**Fig. 2** $(C - C_0)$ / $(\tau - \tau_0)$ against $(C - C_0)$ for AmDec (△) (pH 9.2, $I$ = 0.1) and AmDodec (○) (pH = 9.8, $I$ = 0.1)

$$P(Q) = [3(\sin QR - QR\cos QR)/QR)^3]^2 \quad (4)$$

Since $P(Q) = 1.0$ at $Q = 0$, for this condition Eq. (3) can be written in the form,

$$[d\Sigma(0)/d\Omega]^{1/2} = V_p N_p^{1/2}(\rho_p - \rho_m) \quad (5)$$

and hence from a plot of $[d\Sigma(0)/d\Omega]^{1/2}$ against $\rho_m$, the coherent neutron scattering length of the micellar species can be determined from the value of $\rho_m$ when $[d\Sigma(0)/d\Omega]^{1/2}$ goes to zero. The coherent scattering length of the decanoate ion was determined previously [5] using this procedure and gave good agreement with theoretical expectations as shown in Table 3.

The results obtained for AmDodec in $H_2O$-$D_2O$ mixtures are shown in Fig. 3; these results gave $0.15 \pm 0.05 \times 10^{10}\,cm^{-2}$ as a value for $\rho_p$. This compares favourably with the calculated value of $0.1119 \times 10^{10}\,cm^{-2}$. The coherent scattering lengths for all the materials used in the present work are summarised in Table 3.

On conversion of $V_p$ into the molecular mass of the micelle, $M_{mic}$, Eq. (3) can be rewritten as,

$$M_{mic} = N_{AV} d^2 \frac{d\Sigma(0)}{d\Omega} / [(C - C_0)(\rho_p - \rho_m)^2] \quad (6)$$

with $d =$ the density of the micelle and $(C - C_0)$ the concentration of the micellar species expressed as a monomer, as used for light scattering.

However, when there are interactions between the micelles Eq. (4) needs to be written in the form,

$$M_{mic} = N_{AV} d^2 \frac{d\Sigma(0)}{d\Omega} / [(C - C_0)(\rho_p - \rho_m)^2 S(0)] \quad (7)$$

with $S(0)$ the value of the structure factor, $S(Q)$, at $Q = 0$. Also, as $(C - C_0)$ tends to 0 so $S(Q)$ tends to 1.0. Moreover, $S(0) = kT/(d\pi/N_p)_T$ with $(d\pi/dN_p)_T$ the osmotic compressibility [28] and hence $S(0)$ is directly linked to the second virial coefficient $B$ used in Eq. (1).

*Ammonium decanoate*

As shown in previous work using SANS [5] the experimental data for AmDec could be fitted using the shape factor for a spherical micellar unit; the fit is illustrated in Fig. 4a. The radius of the micellar unit was found to be 17.8 Å and the mean micellar mass was

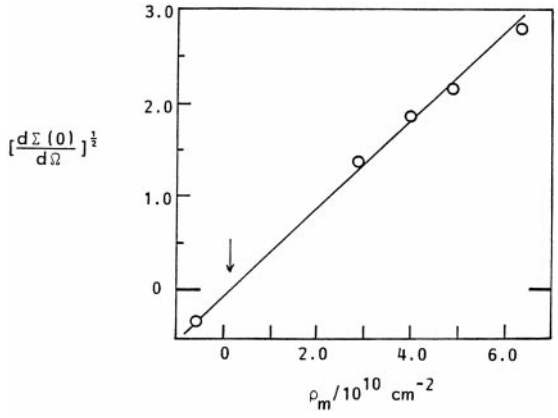


**Fig. 3** $[d\Sigma(0)/d\Omega]^{1/2}$ against $\rho_m$ for 0.1 mol dm$^{-3}$ AmDodec in $H_2O$ : $D_2O$ mixtures at pH 9.8, $I = 0.1$

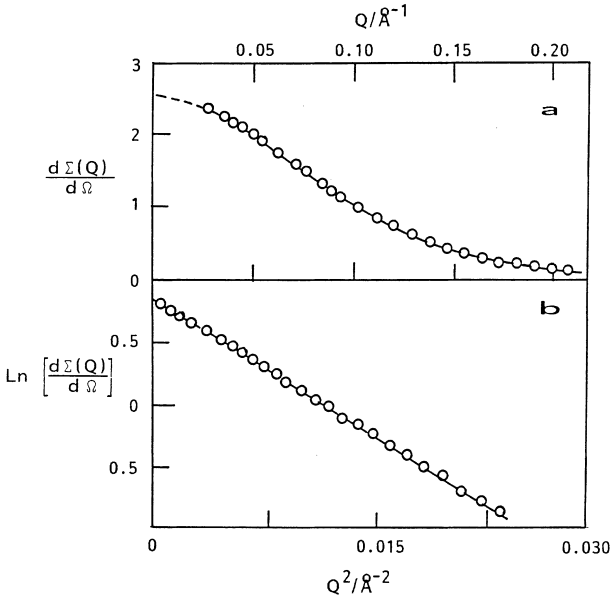


**Fig. 4** Small-angle neutron scattering results for AmDec (0.15 mol dm$^{-3}$) at pH = 9.2, $I$ = 0.1 **a** $[d\Sigma(Q)/d\Omega]$ against $Q$; fitted curve for sphere, R = 17.8 Å. **b** ln $[d\Sigma(Q)/d\Omega]$ against $Q^2$

**Table 3** Coherent neutron scattering length densities, $\rho$

| Material | Formula | $M$/g mol$^{-1}$ | Density/g cm$^{-3}$ | $\rho/10^{10}$ cm$^{-2}$ |
|---|---|---|---|---|
| Water | $H_2O$ | 18.02 | 0.997 | −0.56 |
| Deuterium oxide | $D_2O$ | 20.03 | 1.107 | 6.35 |
| Decanoate | $C_9H_{19}COO^-$ | 171.3 | 0.886[b] | 0.22[a] |
| Dodecanoate | $C_{11}H_{23}COO^-$ | 199.3 | 0.868[b] | 0.19[c] |

[a] Calculated value, experimental = $0.25 \pm 0.05 \times 10^{10}$ cm$^{-2}$ [5]
[b] Acid values-Am salt values were not available
[c] Calculated value, experimental = $0.13 \pm 0.05 \times 10^{10}$ cm$^{-2}$

$10,600 \pm 500$, using Eq. (4). Thus the results obtained from both light scattering and neutron scattering appear, within experimental error, to be in quite good agreement. Moreover, with AmDec the Guinier plots of $\ln[d\Sigma(0)/d\Omega]$ against $Q^2$ were quite linear in the low $Q$ region followed by deviations from linearity in the negative direction (see Fig. 4b); this supports the probability of a spherical shape.

*Ammonium dodecanoate*

The SANS data obtained on AmDodec solutions at concentrations of 0.01, 0.02, 0.05, 0.075 and 0.10 mol $dm^{-3}$, at pH 9.8 and $I = 0.1$ are presented in Fig. 5 in the form of $\ln[d\Sigma(Q)/d\Omega]$ against $Q^2$, i.e. as Guinier plots for the low $Q$ region. At the lowest concentration the plot is reasonably linear with a small upturn at very low $Q$ values. As the concentration increases, however, the low $Q$ region shows a distinct upturn which becomes more significant as the concentration increases. An extended $\ln[d\Sigma(Q)/d\Omega]$ against $Q^2$ plot for the lower concentrations of 0.01 and 0.02 mol $dm^{-3}$ (Fig. 6) shows that at 0.01 mol $dm^{-3}$ the curve tends downwards below the "linear" region. At a concentration of 0.02 mol $dm^{-3}$, however, the line in the higher $Q$ region bends upwards above the "linear"

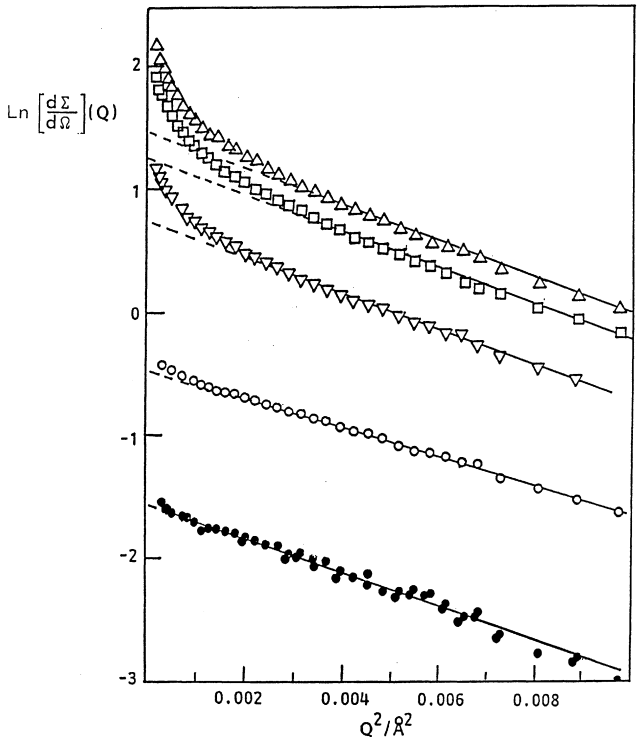


**Fig. 5** $\ln[d\Sigma(Q)/d\Omega]$ against $Q^2$ for AmDodec (pH = 9.8, $I = 0.1$) at various concentrations/mol $dm^{-3}$ : ●, 0.010 ○, 0.020; ▽, 0.050; □, 0.075; △, 0.10

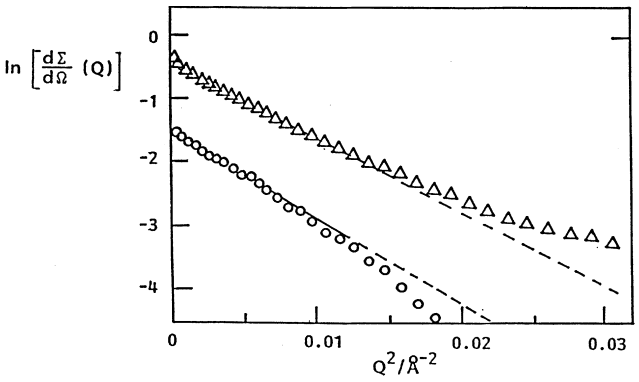


**Fig. 6** $\ln[d\Sigma(Q)/d\Omega]$ against $Q^2$ for AmDodec (pH = 9.8, $I = 0.1$) at concentrations/mol $dm^{-3}$ : ○, 0.010; △, 0.02

line; in addition there is a distinct rise in the region where $Q$ approaches 0.

These indications suggested that unlike the situation with AmDec, where all the evidence is in favour of spherical micelles at the concentrations examined, with AmDodec the increase in scattering in the lower $Q$ region is consistent with the presence of a larger dimension that increases with increasing concentration [27]. Since the results for AmDodec could not be fitted using the shape factor for a spherical micelle or a polydisperse distribution of spherical micelles, except for a possibility at 0.01 mol $dm^{-3}$ the possibility of cylindrical micellar units was investigated.

For a homogeneous right circular cylinder of length $2H$ and radius $R$ the shape factor, $P(Q)$, is given by

$$P(Q) = \int_0^{\pi/2} \frac{\sin^2(QH\cos\beta)}{Q^2H^2\cos^2\beta} \frac{4J_1^2(QR\sin\beta)}{Q^2R^2\sin^2\beta} \sin\beta \, d\beta \qquad (8)$$

where $\beta$ is the angle between the axis of the cylinder and the bisectrix [29] and $J_1(QR\sin\beta)$ is a Bessel function of order 1 [30].

For a detailed examination of the data eq. (8) was used in combination with the least-squares fitting technique "FITFUN" [31] to correlate the experimental results with values of the half-length, $H$, and the radius of the cylinder, $R$. The best fits to the data were obtained using a constant radius of 15 Å and allowing $H$ to vary. This indicated that $H$ increased with the concentration of AmDodec. At the lowest concentration the data could also be fitted to a spherical shape but the radius derived appeared large, $24.1 \pm 0.5$ Å, compared with the length of the dodecyl chain. In fact, a cylinder of small $H$ may be difficult to distinguish from a spherical unit. However, in view of the results at higher concentrations the cylindrical interpretation was preferred.

The fits to the data using a cylindrical model are shown in Figs. 7 and 8. The values of $H$ and $R$ obtained from the fits are given in Table 4. From these data the

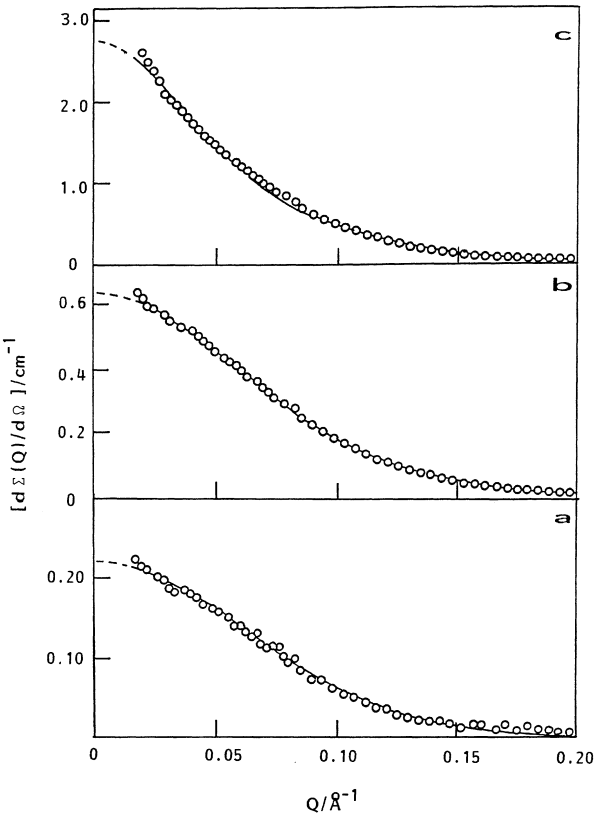


**Fig. 7a-c** [$d\Sigma(Q)/d\Omega$] against $Q$ for AmDodec (pH = 9.8, $I$ = 0.1) at various concentrations/mol dm$^{-3}$: **a** 0.01; **b** 0.02; **c** 0.05. The solid line is the fitted curve for cylinders

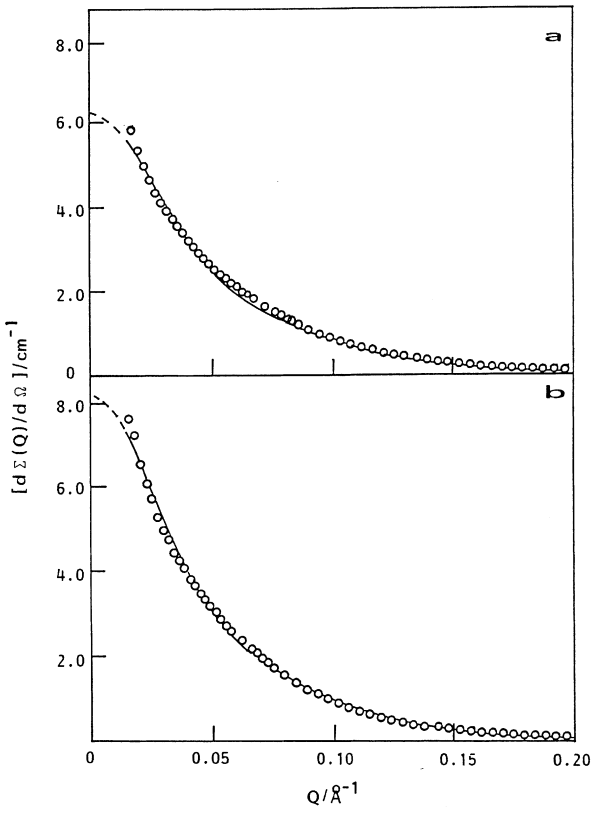


**Fig. 8a,b** [$d\Sigma(Q)/d\Omega$] against $Q$ for AmDodec (pH = 9.8, $I$ = 0.1) at various concentrations/mol dm$^{-3}$: **a** 0.075; **b** 0.10. The *solid line* is the fitted curve for cylinders

**Table 4** Shape results for AmDodec

| Concentration mol dm$^{-3}$ | $H$/Å | $R$/Å | $V_p$/Å$^3$ | $R_g$/Å | $M_{mic}$ /g mol$^{-1}$ |
|---|---|---|---|---|---|
| 0.010 | 28.4 | 15.0 | 40 155 | 19.5 | 20 982 |
| 0.020 | 29.3 | 15.0 | 41 427 | 20.0 | 21 647 |
| 0.050 | 46.6 | 15.0 | 65 888 | 29.0 | 34 429 |
| 0.075 | 61.6 | 15.0 | 87 096 | 37.1 | 45 511 |
| 0.100 | 67.1 | 15.0 | 94 873 | 40.2 | 49 575 |

**Table 5** $M_{mic}$ values from Fig. 9

| $(C-C_0)$/g cm$^{-3}$ | $d\Sigma(0)/d\Omega$ cm$^{-1}$ | $M_{mic}$/g mol$^{-1}$ |
|---|---|---|
| 0.00233 | 0.653 | 34 000 ± 3000 |
| 0.00889 | 2.87 | 39 000 ± 3000 |
| 0.01429 | 6.19 | 52 000 ± 3000 |
| 0.01972 | 8.20 | 50 000 ± 3000 |

volume of the corresponding cylindrical unit was calculated; then using the density of dodecanoic acid (Table 1) the mass and hence the micellar mass were calculated. It is clear that the latter increases with concentration and this explains the form of the turbidity against concentration curves (Fig. 1). Moreover, the light scattering molecular mass obtained by extrapolation to zero $(C - C_0)$ is a weight-averaged value and is clearly influenced by the results at higher concentrations. It would appear that the decrease of the $(C - C_0)/(\tau - \tau_0)$ values at higher concentrations (Fig. 2) is a consequence of increasing micellar mass.

For a sphere of radius $R$ the radius of gyration is given by $R_g^2 = 3R^2/5$, whereas for cylinder of length $2H$ and radius $R$ it is given by [27]

$$Rg^2 = R^2/2 + H^2/3.$$

Values of $R$ as calculated from the fits of $H$ and $R$ are also given in Table 4.

From the fits to a cylindrical model it was also possible to obtain values of $d\Sigma(0)/d\Omega$ and hence to make use of Eq. (5). The results obtained expressed in the form of $(C - C_0)/[d\Sigma(0)/d\Omega]$ against $(C - C_0)$ are plotted in Fig. 9; $[d\Sigma(0)/d\Omega]_{cmc}$ was identical with that of the solvent. The lowest concentration measured, 0.01 mol dm$^{-3}$, was not used as it was too close to the

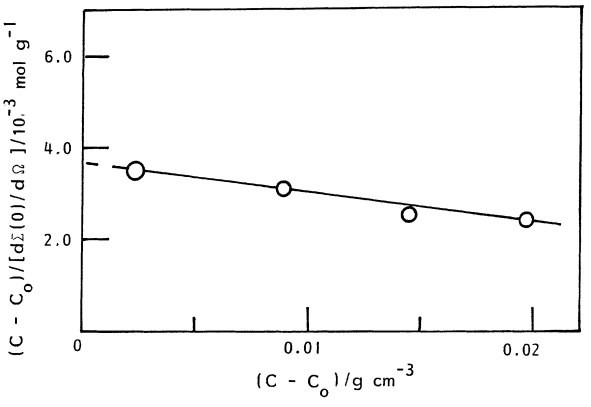


**Fig. 9** $(C - C_0)/[d\Sigma(0)/d\Omega]$ against $(C - C_0)$ for AmDodec at pH 9.8, $I = 0.1$

cmc to obtain an accurate value of $(C - C_0)$. Extrapolation to zero $(C - C_0)$ gave a weight-averaged value of $M_{mic}$ of 36 200 ± 2,000. An interesting feature of the plot is the negative slope which could be taken to indicate intermicellar attraction. However, it is also consistent with an increasing micellar mass with increasing concentration of surfactant. If the value of $M_{mic}$ is calculated at each point, as shown in Table 5, then a clear indication of increasing micellar mass is obtained. Moreover, the values obtained are reasonably consistent with those obtained from the fits to a cylindrical model for the micelle given in Table 4.

The values at higher concentrations are close to the weight-averaged values obtained from light scattering.

## Discussion

### TLS and SANS

The results for AmDec and AmDodec are compared in Fig. 2. AmDec displays a turbidity/concentration profile typical of a surface active agent for which the micelle size above the cmc is approximately constant, with deviations from linearity to lower turbidity values being explained by micelle-micelle interactions. The micellar mass of AmDec of 10 200 from these light-scattering data is in good agreement with the value obtained from SANS of 10 600.

Whilst AmDec forms a spherical micelle with little variation in aggregation number with concentration, AmDodec appears to prefer a cylindrical micelle conformation under the applied pH and ionic strength conditions investigated. Micelle growth has been shown to occur with increasing surfactant concentration with a concommittant increase in the average length of the cylinders. The radius appears to remain essentially constant.

Following the treatment of Hermans and Prins [31] Eq. 1 can also be written in the form,

$$H(C - C_0)/(\tau - \tau_0) = [1 + p^2(C - C_0)/\{2xM + p(C - C_0)\}]/M, \quad (9)$$

where $p$ is the effective charge on the micelle and $x$ is the concentration of 1.1 electrolyte including the monomeric surfactant; the term in square brackets is the second virial coefficient term, $2B$ (cf. Eq (1)).

Hence, it follows that

$$\{d[H(C - C_0)/(\tau - \tau_0)]/d(C - C_0)\}_{c\to 0} = p^2/2xM^2, \quad (10)$$

so $p$ can be estimated from the gradient of the curve of $H(C - C_0)/(\tau - \tau_0)$ against $(C - C_0)$.

Moreover, since $N = M_{mic}/M_{mon}$ the association number, $N$, can also be obtained and hence the ratio $p/N$, the fractional charge on the micelle.

For AmDec $B$ was found to be $0.76 \times 10^{-3}$ mol cm$^3$ g$^{-2}$ which gave $p = 5.62$. Hence, taking the monomer unit in the micelle as having a molecular weight of 189.2 (AmDec) and using the light-scattering value of $M_{mic}$, namely 10,200, we find $N = 54$ for the association number and $p/N = 0.10$. Moreover, using 0.886 for the density of AmDec gives a micellar volume of $1.912 \times 10^{-20}$ cm$^3$ and a radius of 16.6 Å, which with $N = 54$ gives an area per head group on the spherical micelle of 64 Å$^2$.

Since, for a spherical unit the surface charge density, $\sigma$, is given by

$$\sigma = pe/4\pi R^2 \quad (11)$$

we find $\sigma = 2.60 \times 10^{-2}$ Cm$^{-2}$ for $p = 5.62$, $e = 1.6 \times 10^{-19}$ C and $R = 16.6$ Å. Moreover, since

$$\Psi = \sigma R/\epsilon_r\epsilon_0(1 + \kappa R) \quad (12)$$

with $\epsilon_r$ = the relative permittivity of water, $\epsilon_0$ = the permittivity of free space, $\Psi$ = the surface potential of the micelle and $\kappa$ the Debye-Hückel reciprocal length, $\Psi$ can be estimated. For AmDec this gives a $\Psi$ value of 23 mV.

For AmDodec $B = 1.259 \times 10^{-3}$ mol cm$^3$ g$^{-2}$ which gives $p = 35.5$. For the light-scattering $M_{mic}$ value of 57 800 and taking the monomer unit in the micelle as having a molecular weight of 217.6 gives $N = 265$ and $p/N = 0.13$. The value of $B$ was taken from the initial slope of Fig. 2 since, from the definition of $B$, with increase of micellar mass $B$ should decrease in magnitude [28].

Taking the area of a cylinder as $4\pi RH$ with $R = 15$ and $H = 67.1$ Å gives 48 Å$^2$ for the area per head group. If the ends are also included then the total area is 14,063 Å$^2$ and the area per head group = 53 Å$^2$.

For the cylindrical micelle the surface charge density obtained as above, but using the surface area of a cylinder, is $4.04 \times 10^{-2}$ Cm$^{-2}$. For a long cylinder the diffuse layer potential is given by [33],

$$\Psi = RH\sigma f(\kappa R)/\epsilon_r\epsilon_0(H + R)\kappa R, \quad (13)$$

where $f(\kappa R)$ is a quotient of Bessel functions, the values of which have been tabulated by Abramson and Hunter [33, 34]. Hence, taking $R = 15$ Å and $H = 67.1$ Å gives $\Psi = 37$ mV.

These figures suggest a similar degree of surface ionisation and surface potential for both AmDec and AmDodec despite the differences in geometry. Also, the inferred degree of ion-binding for the ammonium counterions is quite similar to that found for other associated surfactants [2, 35]. Moreover, since the extent of ion binding is very similar the implication is that the micellar shape change between the $C_9$ and $C_{11}$ alkyl chains is not a function of ion binding.

An interesting comparison between the SANS results and the data from TLS arises from the different ratio of wavelength $\lambda_0$ used to characterise size by the two techniques. The ratio $Rn_0/\lambda_0$ decreases from 1.7 to 0.0051 (taking $R$ as 16.6 Å) and hence little variation of the measured intensity with angle is expected for light scattering whilst SANS is sensitive to the shape of the micelles with substantial variation of intensity. The range of $Q$ accessible to each experiment alters the sensitivity of the data to different components of the structure. For rods the smaller dimension $R$ will be significant at large $Q$ while the length will dominate at small $Q$. Although both SANS and light scattering will provide a weight-averaged micellar mass, if the range of momentum transfer is limited the result may be biased by the range of $Q$ measured. Light scattering at $Q = 0.0027$ Å$^{-1}$ will be sensitive to the largest dimension and may include large values of $H$ that are missed by the SANS data. It is clear from the data for AmDodec that large values of $H$ are found at higher concentrations but $R$ remains essentially constant. This effect may be particularly important if there is some distribution of the length of micelles and would give rise to a higher average micellar mass being observed by light scattering.

## Geometric considerations

Tanford [36] gives the following expression for the maximum length of an alkyl chain, $l_{\max}$, in Ångstroms

$$l_{\max} = 1.5 + 1.265n_c' \quad (14)$$

where $n_c'$ represents the number of carbon atoms in the hydrocarbon chains that are embedded in the hydrophobic micelle core; this is a figure which can be less than the total number of carbon atoms in the chain. For a micelle containing $N$ hydrocarbon chains Tanford also gives an expression for the volume of the micelle, namely,

$$V_{\text{mic}} = (27.4 + 26.9n_c')N \quad (15)$$

with the numerical values in brackets taken from the data of Reiss-Husson and Luzzati [37]. From these expressions taking $n_c' = 10$ we find $l_{\max}$ 14.1 Å and $V_{\text{mic}} = 16\,006$ Å$^3$ which can be compared with the values of 16.6 Å for $R$ and 19 120 Å$^3$ derived earlier for AmDec from the light-scattering $M_{\text{mic}}$ of 10,200. Tanford also emphasizes that these calculated values are more likely to be the dimensions of the hydrocarbon core rather than the total micelle. Indeed, if the length of a C—O bond, 1.26 Å, is added to 14.1 Å the chain length is extended to 15.4 Å in the dry state, which allowing for ±1 Å in the experimental data can be considered quite good agreement. The value of 17.8 Å, obtained from SANS using a Guinier analysis [27] must also include some contribution from the counter ions on the surface of the micelle since the $p/N$ values indicate extensive ion binding; it will also include any surface roughness.

The idea, based on geometrical arguments, that there is a maximum number of alkyl chains which can be contained in a spherical unit is also discussed by Tanford. He suggests for $n_c' = 10$ a value of 40 and for $n_c' = 12, 54$. In a more detailed geometrical argument Israelachvili et al. [38] suggested that for a spherical unit, $R$ should be of the order $3V/A_0$ with $V$ the volume of the hydrocarbon tail group and $A_0$ the head group area. For AmDec taking $V = 321.1$ Å$^3$ and $A_0 = 64$ Å$^2$ gives $R = 15.1$ Å in reasonable agreement with the figures quoted above. Thus geometrical arguments support the case for a spherical micelle and it seems reasonable to conclude that for AmDec the micelles formed, up to a solution concentration of 0.14 mol dm$^{-3}$, have a spherical shape.

In the case of AmDodec the association number, from SANS data, varies from 95 to 228 over the concentration range examined. These values are well above the value of 54 suggested by Tanford as the maximum for a spherical micelle with $n_c' = 12$. The arguments of Israelachvili et al. [38] suggest that for a cylindrical unit, $R$ should be of the order $2V/A_0$ and from $V = 416.4$ Å$^3$ with $A_0 = 59$ Å$^2$ we find 14.1 Å. The latter is close to the value of 15.0 Å observed experimentally. Thus the evidence, from a detailed analysis of the SANS data, that AmDodec forms cylindrical micelles which increase in length with a constant radius is supported by geometrical arguments.

The significant growth of AmDodec micelles with increased concentration by elongation of the cylinder has been observed for other surfactants which form rod-shaped micelles [11, 12, 39], and suggests that micellar growth is energetically more favourable for cylinders than spheres.

Sodium dodecyl sulphate forms spherical micelles of radius 23-27 Å in water [7] but with addition of sodium chloride at 0.4 mol $dm^{-3}$ undergoes a sphere-to-cylinder transition. This compares with the fact that AmDodec needs an ionic strength of only 0.1. It can be anticipated that the effect of added salt is to reduce repulsion between the charged head groups thus reducing $A_0$ and favouring cylindrical geometry. It also implies that carboxylate head group repulsions are inherently smaller than those of the sulphate group, a large "hydrophilic" ion [40].

Increasing the alkyl chain length also leads to ellipsoidal/cylindrical micelles as shown with sodium hexadecyl sulphate [41].

It is also interesting to speculate that the formation of cylindrical micelles is a precursor state for the formation of a middle phase which consists of hexagonally packed cylinders [42].

## Thermodynamic arguments

Tail effects on the free energy of micellisation have been modelled by Puvvada and Blankschtein [43]. By computation of all possible tail-group conformations in the micelle and a model calculation of the corresponding free energy, they have determined the optimum minor radius of the micelle $R_{opt}$ to give the minimum free-energy for each possible micellar shape. The model predicts that $R_{opt}$ is less if a given surface active agent forms a cylindrical rather than a spherical micelle, and indicates that for a surfactant such as *n*-dodecyl hexaoxyethylene glycol monoether ($C_{12}E_6$), the free-energy minimum corresponding to a cylindrical micelle is less than that for a spherical micelle, implying that a cylinder is the preferred shape, as shown experimentally [44]. A full explanation as to why AmDodec prefers to form cylindrical micelles will similarly require a detailed model of all the free-energy contributions of headgroups and tailgroups in micellisation. An additional explanation for cylindrical micelles being preferred by higher members of a homologous surfactant series is that the fully extended chain becomes energetically less favoured as the chain length increases.

**Acknowledgements** We wish to thank Procter and Gamble Limited for support of this work. We also wish to thank EPSRC for support of R.M.C. and the Institut Laue Langevin for the use of neutron facilities. R.H.O. and A.R.R. also thank the DTI colloid technology programme for support.

## References

1. Tanford C (1980) The hydrophobic effect, 2nd edn. Wiley, New York
2. Ford WPJ, Ottewill RH, Parreira HC (1966) J Colloid Interface Sci 21: 522
3. Reiss-Husson F, Luzzati V (1964) J Phys Chem 8: 3504
4. Neesorn PC, Jennings BR, Tiddy GJT (1983) Chem Phys Lett 95: 533
5. Burkitt SJ, Ottewill RH, Hayter JB, Ingram BT(1987) Colloid Polym Sci 265: 619
6. Hoffmann H, Kalus J, Reizlein K, Ulbricht W, Ibel K (1982) Colloid Polym 260: 435
7. Hayter JB, Penfold J (1983) Colloid Polym Sci 261: 1022
8. Anacker EW (1979) In: Mittal KL (ed) Solution chemistry of surfactants. Plenum, NewYork, p 247
9. Mazer NA, Benedek CB, Carey MC (1976) J Phys Chem 80:1075
10. Imae T, Kamiya R, Ikeda S (1985) J Colloid Interface Sci 108:215
11. Ulmins J, Wennerstrom H (1977) J Maq Reson 28: 309
12. Lessener E, Frahm J (1982) J Phys Chem 86:15
13. Hayter JB, Penfold J (1981) Mol Phys 42: 109
14. Burkitt SJ, Ottewill RH, Hayter JB, Ingram BT (1987) Colloid Polym Sci 265: 628
15. Burkitt SJ, Ingram BT, Ottewill RH (1988) Prog Colloid Polym Sci 76:247
16. Clapperton RM, Ingram BT, Ottewill RH, Rennie AR (1992) ACS Symp Ser 501: 268
17. Clapperton RM, Ottewill RH, Ingram BT (1994) Langmuir 10: 51
18. Clapperton RM, Ottewill RH, Rennie AR (to be published)
19. Ibel K (ed) (1994) Guide to neutron research facilities at the ILL. Institut Laue Langevin, Grenoble
20. Jacrot B (1976) Rep Prog Phys 39: 911
21. Brice BA, Halwer M, Speiser R (1950) J Opt Soc Amer 40: 768
22. Kerker M (1969) The scattering of light. Academic Press, New York
23. Kratohvil JP, Dezelić G, Kerker M, Matijević E (1962) J Polym Sci 57: 59
24. International Critical Tables (1930) VII: 75
25. Debye P (1949) J Phys Colloid Chem 53: 1
26. International Critical Tables (1930) VII: 13
27. Guinier A, Fournet G (1955) Small-angle scattering of X-rays. Wiley, New York
28. Ottewill RH, Richardson RA (1982) Colloid Polym Sci 260: 708
29. van de Hulst HC (1957) Light scattering by small particles. Wiley, New York
30. Abramowitz M, Stegun IA (1968) Handbook of mathematical functions. Dover, New York
31. Ghosh R (1989), FITFUN – an interactive/graphical fitting routine, report No 89GH08T. Institut Laue Langevin, Grenoble
32. Prins W, Hermans JJ (1955) J Phys Chem 59: 576
33. Abramson HA (1942) Electrophoresis of proteins. Hafner, New York.
34. Hunter RJ (1981) Zeta potential in colloid science. Academic Press, London, p 30
35. Hunter RJ (1987) Foundations of colloid science, vol 1. Clarendon Press, Oxford, p 598
36. Tanford, C (1973) The hydrophobic effect. Wiley, New York
37. Reiss-Husson F Luzzati V (1966) J Colloid Interface Sci 21: 534

38. Israelachvili JN, Mitchell PJ, Ninham BW (1976) J Chem Soc Faraday Trans II 72: 1525
39. Bendedouch D, Chen S (1984) J Phys Chem 92: 3710
40. Bongiovanni R, Ottewill RH, Rennie AR, Laughlin RG (1996) Langmuir 12: 4681
41. Borbely S, Cser L, Bezzabotnov VY, Ostanevich YM et al (1993) Colloid Polym Sci 271: 786
42. Laughlin RG (1994) The aqueous phase behaviour of surfactants. Academic Press, London
43. Puvvada S, Blankschtein D (1990) J Chem Phys 92: 3710
44. Cebula DJ, Ottewill RH (1982) Colloid Polym Sci 260: 1118